JURNAL KIMIA VALENSI
p-ISSN: 2460-6065; e-ISSN: 2548-3013
Journal homepage: https://journal.uinjkt.ac.id/index.php/valensi

Research Article

Fabrication of Calcite Calcium Carbonate from Eggshells Biogenic Waste Through Carbonation Method

Mariyam Mariyam[1], Siti Sunarintyas[2], Leny Yuliatun[3], Ismi Khuzaimah[4] and Nuryono Nuryono[4*]

[1]Department of Chemistry, Faculty of Science, Institut Teknologi Sumatera, South Lampung, 35365, Indonesia
[2]Department of Dental Biomaterial, Faculty of Dentistry, Universitas Gadjah Mada, Sleman, 55281, Indonesia
[3]Research Center for Biomass and Bioproduct, National Research and Innovation Agency, Cibinong, 16911, Indonesia
[4]Department of Chemistry, Faculty of Mathematics and Natural Sciences, Universitas Gadjah Mada, Sleman, 55281, Indonesia

[*]Email: nuryono_mipa@ugm.ac.id

Article Info
Received: Oct 18, 2024
Revised: Feb 11, 2025
Accepted: Marc 8, 2025
Online: May 31, 2025

Citation:
Mariyam, M., Sunarintyas, S., Yuliatub, L., Khuzaimah, I., & Nuryono, N. (2025). Fabrication of Calcite Calcium Carbonate from Eggshells Biogenic Waste Through Carbonation Method. *Jurnal Kimia Valensi*, 11(1), 9-17.

Doi:
10.15408/jkv.v11i1.41914

Abstract

Calcium carbonate derived from eggshells has significant potential for use in drug delivery systems, pharmaceutical, food, catalyst, cement, and concrete industries. Although eggshell waste is non-toxic, its excessive accumulation in the environment may contribute to ecological issues. Colonizing pathogenic bacteria in unprocessed eggshell waste poses a potential health risk. The present study outlines the production of precipitated calcium carbonate (PCC) from eggshell waste through a calcination-carbonation process, offering a sustainable approach to its utilization. The calcination was carried out at 900 ºC. The carbonation process was performed in an HNO_3 solution, and the NH_3 solution was under-treated for 60 minutes. The results exhibited that the precipitated calcium carbonate (PCC) had a purity of 95.2% CaO. It possessed predominantly the calcite phase with a rhombohedral crystal system, as confirmed by the XRD analysis. The crystallite size of PCC was 109.5 nm, measured using the *Debye-Scherrer* equation. The phase composition of PCC was 99.3% calcite, 0.5% vaterite, and 0.2% aragonite. FTIR analysis further corroborated this data by showing a sharp and unsplit peak at 1419 cm^{-1}, demonstrating the presence of a calcite phase. SEM images revealed a cubic-like morphology, a characteristic of the calcite form of calcium carbonate ($CaCO_3$). The synthesized calcium carbonate in this study holds potential for applications in dental materials and as fillers in polymer matrices for food packaging.

Keywords: $CaCO_3$, calcite, carbonation, eggshell, synthesis

1. INTRODUCTION

Biowaste eggshells are common byproducts of the food industry and domestic consumption, typically considered waste and discarded in large quantities. This considerable eggshell waste contributes to landfill accumulation and environmental degradation. Although eggshell's biogenic waste is not inherently toxic or environmentally hazardous, the decomposition of their inner shell membrane in soil may facilitate the colonization of various pathogenic microorganisms, including *Salmonella* and *Escherichia coli* [1]. Consequently, European Union (EU) regulations classify industrial eggshells byproducts as hazardous biological waste [2]. However, using eggshell waste to produce valuable materials, such as $CaCO_3$, not only offers a solution to waste management issues but also aligns with circular economy principles, promoting sustainability and responsible resource management.

The high calcium carbonate content (approximately 97% by weight) presents a valuable opportunity for resource recovery and sustainable material synthesis [3]. Calcium carbonate can be applied in various fields, including pharmaceuticals, cosmetics, catalysts for biodiesel production, food industries, cement and concrete materials [4–6]. Calcium carbonate is an essential raw material for synthesizing hydroxyapatite in biomedical engineering applications [7]. Additionally, it is utilized as a precursor in the synthesis of calcium silicate, which serves as bone scaffolds and endodontic materials [8–10].

Various methods exist to extract calcium carbonate from biowaste, including chemical leaching, hydrothermal synthesis, and carbonation [11–13]. Among these, the carbonation method is widely recognized for its ability to produce PCC with high purity and yield [12]. The carbonation process involves dissolving calcium oxide (CaO) obtained from the thermal decomposition of $CaCO_3$ in eggshells and allows carbon dioxide (CO_2) to flow through the solution to precipitate $CaCO_3$. The carbonation method allows for the precise control of the crystalline phase, morphology, and particle size of $CaCO_3$, ensuring its suitability for diverse applications [14]. Moreover, the method is known to yield a uniform particle size distribution, which is critical for applications that require specific morphologies and sizes, such as in dental materials and fillers for polymers. This environmentally friendly process operates under mild conditions, without the need for high temperatures or pressures, making it an excellent choice for large-scale $CaCO_3$ production.

The three polymorphic forms of $CaCO_3$ are aragonite, vaterite, and calcite. Aragonite crystallizes in an orthorhombic structure, calcite exhibits a rhombohedral crystal system, and vaterite forms a hexagonal structure. Among these phases, calcite represents the thermodynamically most stable form at ambient temperature [1]. The calcite phase is the most suitable material for applications, including biosensors, photocatalysts, and drug delivery systems, due to its higher thermodynamic stability compared to the other two polymorphs. Pyrazino isoquinoline-loaded $CaCO_3$ has enhanced water solubility and hydrophobic characteristics, making it a promising candidate for drug delivery systems [15]. Bikharudin et al. (2022) has synthesized PCC from lime stone by dissolving the sample with high concentration of HNO_3 (1M) followed by carbonation for 30 min without involving the calcination [16]. To the best of our knowledge, the synthesis of calcite $CaCO_3$ from biomass has been relatively underexplored in the literature. Most studies on the synthesis of PCC have primarily employed the calcination method. This approach has been reported to obtain $CaCO_3$ with relatively low purity ranging from 73% to 90%, along with a mixture of different $CaCO_3$ phases [17]. Therefore, this study aims to synthesize calcite calcium carbonate using the carbonation method to obtain $CaCO_3$ with high purity.

2. RESEARCH METHODS

Materials

The materials used in this research were chicken eggshells (collected from a street vendor in Sleman district, Yogyakarta, with good condition, neither rotten nor discolored), nitric acid 65% (Merck), ammonia solution 25% (Merck), universal indicator strips pH 0-14 (Merck), CO_2 gas (99% purity), and deionized water.

Instrumentations

Instrumentations used included Shimadzu prestige 21 Fourier Transform Infrared Spectrophotometer (range 400−4000 cm^{-1}) for functional group determination, an X-Ray diffractometer (XRD) PANalytical X'Pert3 Powder with a scan range of 5-60º for phase identification, an X-ray fluorescence (Rigaku Nex CG II) for multi-elemental composition analysis, and a JSM 6510LA Scanning Electron Microscope (SEM) which operates at an accelerated voltage of 10 kV to examine morphological features.

Preparation of eggshell ash

Eggshells were washed with water, and inner shell membranes were removed. 200 g of cleaned eggshell samples were dried at 100 ºC for 30 minutes, then grounded and subjected to calcination at 900 ºC for 4 hours. The eggshell ash was subsequently sieved through a 200 mesh sieve to achieve small particle sizes.

Synthesis of calcium carbonate

Eggshell ash was dispersed in nitric acid (HNO_3) 0.8 M and stirred continuously for 30 min. The mixture was filtered, and the filtrate was carefully treated with a few drops of 25% ammonia (NH_3) solution. The pH was adjusted to 11-12 to create an alkaline environment. The carbonation process flowed CO_2 gas into the filtrate for 60 minutes. During the carbonation, a 25% ammonia (NH_3) solution was gradually added to the filtrate to maintain an alkaline pH throughout the reaction. Upon completion of the carbonation step, the resulting mixture was subjected to a sonication chamber for 30 minutes to enhance dispersion and ensure uniform precipitation. The precipitate was subsequently filtered while a continuous flow of 200 mL of deionized water was applied to wash the product thoroughly. The precipitated calcium carbonate (PCC) was dried at 100°C to remove residual moisture. The resulting product was then characterized using XRF, SEM, FTIR, and XRD instrumentations. % yield of PCC was calculated using equation 1:

$$Yield = \frac{weight\ of\ PCC}{weight\ of\ eggshell} x\ 100\% \qquad (1)$$

3. RESULTS AND DISCUSSION

Calcium carbonate was synthesized from eggshells using the calcination-carbonation method, yielding 78.8%. The calcination process was conducted at 900 °C to eliminate any organic impurities and facilitate the thermal decomposition of calcium carbonate ($CaCO_3$) to obtain calcium oxide (CaO). HNO_3 was used to synthesize $CaCO_3$ to enhance the solubility of metal oxides, particularly CaO. HNO_3 reacts with CaO to form water-soluble calcium nitrate salts. Calcium nitrate reacts with carbon dioxide (CO_2) gas during the carbonation process, precipitating $CaCO_3$. Ammonia (NH_3) was added before and during the carbonation process to maintain the pH of the filtrate in an alkaline condition, which was essential for facilitating the formation of calcium carbonate. Previous investigations revealed that pH influences the nucleation rate and crystal growth of $CaCO_3$ [14] by equations (2), (3), and (4). At higher pH levels, nucleation starts faster, and more CO_2 is absorbed into the solution, shifting the equilibrium toward forming carbonate ions (CO_3^{2-}), as displayed in equation (4). The increasing of CO_3^{2-} concentration in the solution may favor $CaCO_3$ formation. Therefore, the crystal growth was enhanced under these conditions. Higher pH leads to higher supersaturation, which can reduce the induction period (the time before nucleation starts) [18].

$$CO_2(g) + H_2O(l) \rightleftharpoons H_2CO_3(aq) \quad (2)$$
$$H_2CO_3(aq) \rightleftharpoons HCO_3^-(aq) + H^+(aq) \quad \text{(low pH)} \quad (3)$$
$$H_2CO_3(aq) \rightleftharpoons CO_3^{2-}(aq) + 2H^+(aq) \quad \text{(high pH)} \quad (4)$$

The carbonation method is known for its ability to produce PCC with high yield and purity. Additionally, the product obtained through the carbonation method exhibited a homogeneous particle size distribution and allowed control over the crystalline phase and morphology of $CaCO_3$ [12]. After the carbonation process, the sonication treatment was applied to accelerate PCC particle formation nucleation rate. It promotes the efficient dispersion of CO_2 gas throughout the filtrate solution, facilitating its reaction with calcium ions. This sonication process significantly contributes to the PCC particle formation with a smaller and more uniform distribution [19]. Overall, the reactions involved in the synthesis of PCC are consistent with the equations (5), (6) and (7).

$$CaCO_3(s) \rightarrow CaO(s) + CO_2(g) \quad (5)$$
$$CaO(s) + 2HNO_3(aq) \rightarrow Ca(NO_3)_2(aq) + H_2O(l) \quad (6)$$
$$Ca(NO_3)_2(aq) + 2NH_3(aq) + CO_2 + 3H_2O(l) \rightarrow CaCO_3(s) + 2NH_4NO_3(aq) + 2H_2O(l) \quad (7)$$

According to Altiner et al. (2021), the application of ultrasonic power during PCC synthesis led to the formation of pure calcite crystals instead of a mixture of calcite and vaterite [19]. Ultrasound cavitation generates high temperatures and pressure that increase the nucleation of $CaCO_3$ crystals. Ultrasonic stirring enhances the energy of collisions, promoting rapid transformations and interactions between calcium carbonate polymorphs [20]. Vaterite is formed under conditions of high supersaturations. However, it is metastable and can subsequently transform into aragonite or calcite [21].

Composition of calcined eggshells and eggshells PCC

The composition of calcined eggshells at 900°C (CE900) and precipitated calcium carbonate (PCC) were analyzed by XRF, and the result is presented in Table 1. It indicates that CE900 comprises 87.6% calcium oxide (CaO), with magnesium oxide (MgO) being the most prominent impurity at 7.62%. Following the carbonation process, PCC is formed with a significantly improved purity of 95.2%. Metal oxide impurities are detected at very low concentrations, with percentages lesser than 0.2%. This low concentration of impurities ensures the PCC's high quality and purity, making it a suitable precursor for synthesizing mineral trioxide aggregate (MTA). The high-purity PCC obtained from this process can be used as an ideal precursor for synthesizing medical-grade materials, such as calcium silicate and mineral trioxide aggregate (MTA).

Table 1. Composition of calcined eggshells and precipitated calcium carbonate (PCC)

Oxides Compounds	CE900 (%)	PCC (%)
CaO	87.6	95.2
P_2O_5	0.909	4.144
Fe_2O_3	0.011	0.184
NiO	ND	0.122
CuO	0.007	0.042
ZnO	0.004	0.022
SrO	0.029	0.022
SO_3	0.324	ND
K_2O	0.087	ND
MgO	7.620	ND
Al_2O_3	1.360	ND
SiO_2	0.434	ND

ND: Not Detected

The purity of CaO produced during the synthesis of PCC is affected by various factors, such as pH, acid concentration, and the duration of the carbonation process. During carbonation, the pH is maintained within the range of 11–12 to optimize PCC formation. The high pH level increases the solubility of Ca^{2+} ions, forming more $CaCO_3$ particles [22]. Furthermore, it is noted that the alkaline environment in the PCC synthesis results in the formation of smaller $CaCO_3$ particles.

Functional groups of calcined eggshells and eggshells PCC

CE900 and PCC functional groups were characterized using Fourier Transform Infrared Spectroscopy (FTIR) within the 400–4000 cm^{-1} wavenumber range. The corresponding FTIR spectra are presented in **Figure 1**. The FTIR spectrum of CE900 exhibits a sharp peak at 3641 cm^{-1}, attributed to the stretching vibration of the −OH group bonded to the calcium atom [9]. A broad peak at 3448 cm^{-1} corresponds to the −OH functional groups associated with adsorbed water molecules (**Table 2**). A minor peak at 1797 cm^{-1}, observed in the PCC spectrum and absent in CE900, indicates the C=O stretching vibrations [23]. Sharp peaks are shown in the FTIR spectra of CE900 and PCC at 1442 cm^{-1} and 1419 cm^{-1}, respectively, corresponding to the asymmetric stretching vibrations of the O−C−O bonds in carbonate ions (CO_3^{2-}). The shape of the peak around 1400 cm^{-1} may indicate the specific $CaCO_3$ phase present in materials. A split peak of the CE900 spectrum at 1422 cm^{-1} suggests the presence of a mixture of vaterite and calcite phases [24,25]. Conversely, the PCC spectrum displays a sharp absorption peak at 1419 cm^{-1}, indicating the presence of the calcite phase. The aragonite phase is identified in CE900 at 1049 cm^{-1}, absent in the PCC spectrum [26,27]. Additionally, the presence of CO_3^{2-} ions is confirmed by peaks at 871 cm^{-1} and 709 cm^{-1}, corresponding to out-of-plane and in-plane bending vibrations, respectively. The sharp peak around 709 cm^{-1} further signifies a well-ordered calcite phase [28].

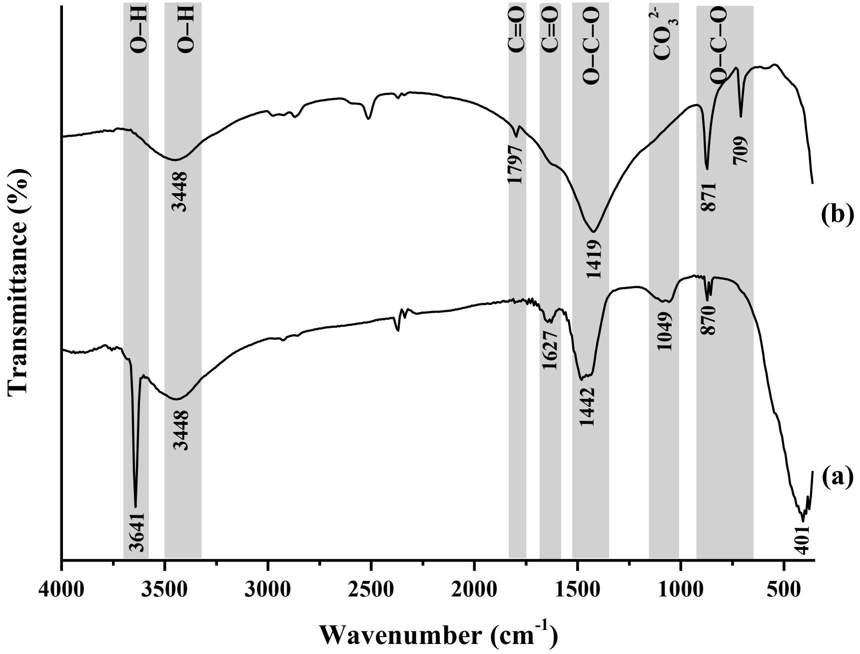

Figure 1. FTIR spectra of (a) CE900 and (b) PCC

Table 2. Functional groups in CE900 and PCC

Wavenumber (cm^{-1})		Functional Groups
CE900	**PCC**	
3641	-	O−H stretching vibration of $Ca(OH)_2$
3448	3448	O–H stretching vibration of H_2O
-	1797	C=O stretching vibration
1627	1627	Carbonyl groups stretching vibration
1442	1419	O−C−O asymmetric stretching vibration of CO_3^{2-}
870	871	Bending vibration of CO_3^{2-} groups (*out of plane*)
-	709	Bending vibration of CO_3^{2-} groups (*in-plane*)

The unsplit peak at 1419 cm^{-1} suggests that the synthesized PCC contains no vaterite phase, typically characterized by a distinct split peak around ~1400 cm^{-1} phases [24,25]. Furthermore, the crystalline phases of aragonite and calcite are differentiated by their absorption features around ~700 cm^{-1}, in which a single sharp peak indicates the calcite phase and two adjacent peaks characterize the aragonite phase [26,28]. Amorphous calcium carbonate, in contrast, is identified by a broad peak with a relatively weak absorption band in this region [26,28]. The application of sonication significantly increases the proportion of the calcite phase relative to the vaterite phase in precipitated calcium carbonate (PCC), as Altiner et al.

(2021) reported. Sonication results in the formation of $CaCO_3$ products with smaller and more uniform particle sizes. It is attributed to the ultrasound waves' micro-level cavitation and diffusion effects, which effectively accelerate the carbonation process [19].

XRD analysis of calcined eggshells and eggshells PCC

The degree of crystallinity and the phases present in eggshells after calcination at 900 °C (CE900) and PCC were characterized using X-ray diffraction (XRD), with the XRD patterns presented in **Figure 2**. The XRD data reveal that CE900 contains $CaCO_3$ in three phases: calcite, vaterite, and aragonite. The vaterite phase is identified by peaks at (2θ) 27.22°, 33.12°, and 50.79°. The aragonite phase is characterized by peaks at (2θ) 26.22°, 38.5°, and 45.83°. PCC diffractogram displays the calcite phase peaks at 2θ angles of 23.11°, 29.44°, 31.47, 36.01°, 39.45°, 43.20°, 47.15°, 47.53°, 48.54°, 56.60°, 57.44°, and 58.11°.

Calcination at 900 °C leads to the formation of CaO, as evidenced by the appearance of peaks at 2θ of 37.88° and 54.3°. Additionally, the presence of portlandite ($Ca(OH)_2$) is detected at (2θ) 18.04°, 28.68°, 34.11°, 47.11°, and 50.78°. The formation of $Ca(OH)_2$ occurs due to the reaction of CaO with atmospheric moisture, resulting in a hydroxylation reaction between CaO and water [29]. CaO is hygroscopic and readily reacts with water vapor from the air upon removal from the furnace.

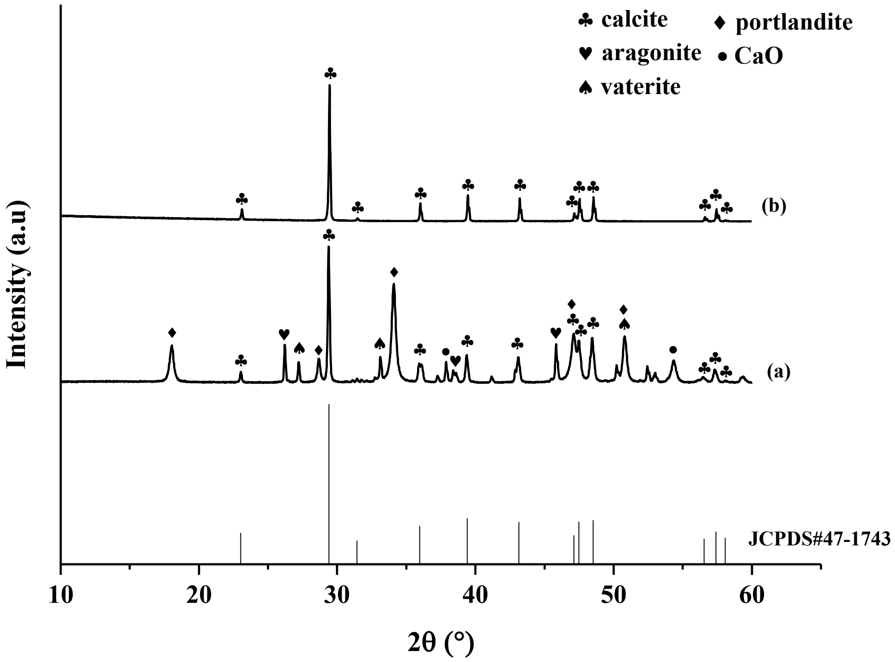

Figure 2. Diffractogram of (a) CE900 and (b) PCC

The XRD analysis confirms that the crystal phase of the synthesized PCC is calcite with a rhombohedral crystal structure. The 2θ peaks observed in the PCC diffractogram correspond to the characteristic peaks of the calcite phase, as verified by comparison with the JCPDS reference standard no. 00-047-1743. According to Othman et al. (2017), calcite is the most thermodynamically stable polymorph of calcium carbonate at ambient temperature and pressure compared to other forms, such as vaterite and aragonite. The XRD data of the synthesized PCC show no evidence of vaterite and aragonite phases, indicating that only the calcite phase is present. The sharp peaks in the PCC diffractogram further indicate that the PCC possesses a high degree of crystallinity.

Analysis was carried out to calculate the phase composition of PCC and CE900 using XRD data. The result shows that the synthesized PCC consists of 99.3% calcite, 0.5% vaterite, and 0.2% aragonite phases, while the calcined eggshell (CE900) consists of 46.7% portlandite, 37.2% calcite, 9.8% aragonite, 5.3% vaterite, and 1.1% CaO as depicted in **Figure 3**. It revealed that the carbonation method applied to synthesized PCC may increase the calcite phase formation of $CaCO_3$ (PCC). During the carbonation process, the phase formation in eggshell-derived PCC synthesis is affected by factors, such as reactant concentration, temperature, and pH. Additionally, the presence of Mg^{2+} ions promotes the formation of metastable aragonite particles, as Mg^{2+} ions may incorporate into the calcite crystal lattice, enhancing calcite solubility at temperatures exceeding 40° [14]. In this study, 0.8 M HNO_3 was utilized to minimize the presence of metal ions during carbonation, resulting in the predominant formation of the calcite phase. Supersaturated $Ca(OH)_2$ concentrations, combined with low temperatures and high pH, are optimal conditions for forming calcite crystals [14]. In contrast, the metastable phases of vaterite and aragonite are more readily formed at lower pH levels and tend to transform into the calcite phase when the pH exceeds 11 during the carbonation process [14].

Calcite is the most thermodynamically stable phase of the $CaCO_3$ polymorphs across various temperatures and pressures. Crystals of the calcite phase are readily synthesized via the carbonation method without additional additives or specific conditions, such as elevated pressure or temperature. Calcite morphology and particle size can be tailored for certain applications by adjusting various synthesis parameters. In dentistry, calcite particles have the potential for use in treating early caries lesions as a calcium source to maintain Ca^{2+} ions in a supersaturated state within tooth enamel mineral, thereby supporting the remineralization process outside the caries lesion. Furthermore, the high stability of the calcite phase enables it to adsorb immunoglobulin Y, enhancing the material's antibacterial properties and potentially preventing dental infection [30].

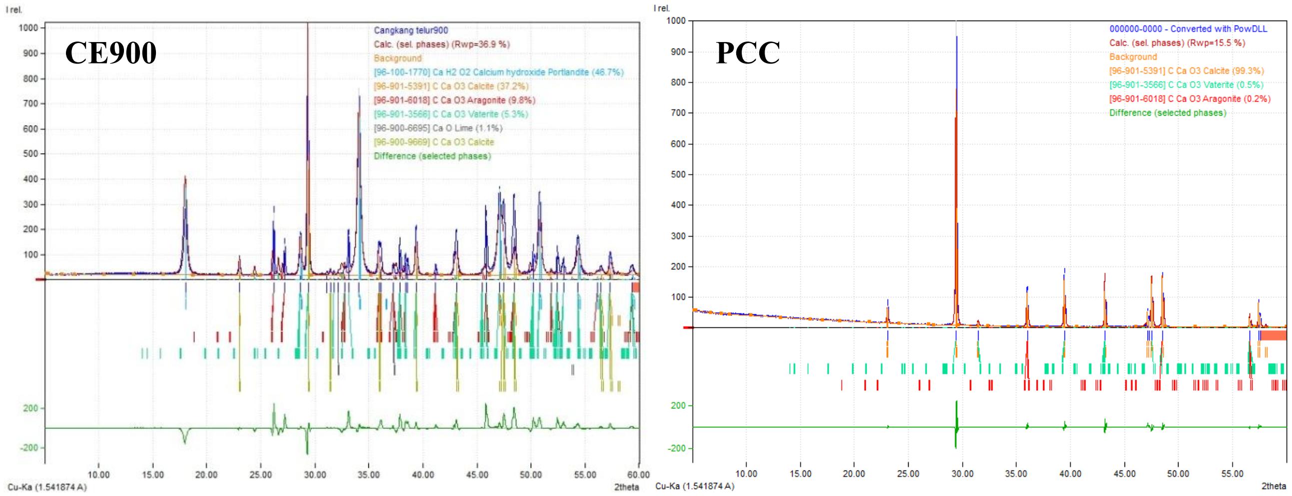

Figure 3. Match! analysis of CE900 and PCC from XRD data

The particle size of $CaCO_3$ is influenced by various factors, including the initial concentration of calcium hydroxide ($Ca(OH)_2$). Higher concentrations of $Ca(OH)_2$ typically result in the formation of larger $CaCO_3$ particles. However, this effect can be resolved by applying sonication treatment during carbonation. Sonication treatment promotes the production of $CaCO_3$ particles with a more uniform size distribution[19]. The average size of PCC crystals can be determined using X-ray diffraction (XRD) data, applying equation 8 (*Debye-Scherrer* equation).

$$D = \frac{K\lambda}{\beta Cos\theta} \tag{8}$$

In this equation, D represents the crystal size, λ is the wavelength of the X-ray radiation (in nm), K is Scherrer's constant (0.9), β denotes the full width at half maximum (FWHM) of the diffraction peak (in radians), and θ is the Bragg angle (in radians). As determined using the *Debye-Scherrer* equation, the average size of the precipitated calcium carbonate (PCC) crystals is 109.5 nm.

Surface morphology of calcined eggshells and eggshells PCC

Scanning Electron Microscopy (SEM) images display the surface morphology of calcined eggshells (CE900) and eggshells PCC as shown in **Figure 4**. The morphology of eggshell ash calcined at 900 °C (**Figure 4a**) reveals a heterogeneous mixture of spherical, irregular, and elongated needle-shaped particles. The variation in particle shape is attributed to multiple crystalline phases, as confirmed by XRD analysis, which identified vaterite, calcite, and aragonite phases in the CE900 sample. In contrast, the morphology of PCC particles (**Figure 4b**) exhibits a well-defined cubic or box-like arrangement, characteristic of the calcite phase, as verified by the XRD diffractogram. SEM images corroborate the characteristic cubic morphology typically associated with $CaCO_3$ calcite.

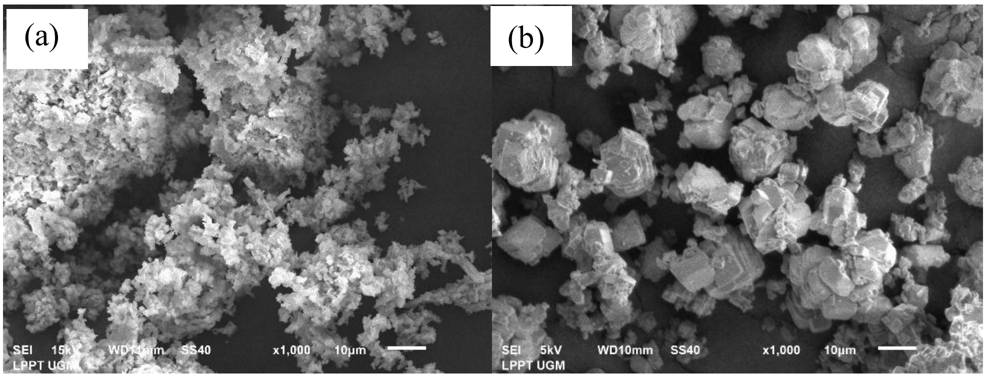

Figure 4. SEM images of (a) CE900 and (b) PCC

Previous studies have reported that calcite typically exhibits a cube-like morphology, vaterite crystals possess a spherical or ball-like structure, and aragonite crystals display an elongated rod or needle-like shape [31]. The phase transformation from vaterite to calcite may occur through a spontaneous recrystallization process or via the dissolution of vaterite particles in aqueous media, as vaterite has a higher solubility in water than calcite. The vaterite-to-calcite phase transformation follows a "relay" recrystallization mechanism, in which metastable particles transform into their stable state through collisions within a stirred suspension[20]. The heat released in the inter-particle contact area during collisions increases the amplitude of thermal vibrations in the atoms, ions, or molecules on the particle surface. This process promotes structural changes, ultimately leading to the transformation from the metastable to the stable phase. Following these collisions, particles may either aggregate or remain as discrete entities. Rapid phase transitions occur in all metastable particles.

Calcite is the most thermodynamically stable $CaCO_3$ polymorph characterized by its low solubility in water and a higher thermal decomposition temperature than vaterite [19]. The stability differences among the three polymorphs, aragonite, calcite, and vaterite, arise from Ca^{2+} and CO_2^{2-} ions arrangements in their solid-state structure [32]. Calcite and aragonite exhibit a staggered arrangement of inter-planar carbonate ions, whereas vaterite is eclipsed relative to each other, contributing to its lower stability. Notably, at temperatures exceeding 380 ºC, aragonite readily transforms into the calcite phase. The superior stability of calcite offers significant advantages for applications such as fillers in plastics or cement, where mechanical strength and uniform stress distributions are crucial [1].

4. CONCLUSIONS

The present study successfully synthesized precipitated calcium carbonate (PCC) from eggshell waste through a calcination-carbonation method, achieving a yield of 78.8%. The XRD analysis confirmed that the synthesized PCC predominantly comprised the thermodynamically stable calcite phase. FTIR spectra further supported this finding, revealing a sharp and unsplit peak at 1419 cm^{-1}. The SEM images demonstrated a well-defined cubic morphology, characteristic of the calcite structure of $CaCO_3$. The purity of the synthesized PCC reached 95.2%, as determined by XRF analysis, making it suitable for use as a precursor in synthesizing high-grade materials such as calcium silicate and mineral trioxide aggregate (MTA). The sonication treatment employed in this study enhanced particle uniformity and accelerated the carbonation process, producing smaller and more uniform PCC particles.

ACKNOWLEDGMENTS

The research was partly financed by the Faculty of Mathematics and Natural Sciences, Gadjah Mada University through the Flagship Research Grant, contract number 2456/UN1/FMIPA.1.3/KP/PT.01.03/2024.

REFERENCES

1. Azarian MH, Sutapun W. Tuning polymorphs of precipitated calcium carbonate from discarded eggshells: effects of polyelectrolyte and salt concentration. *RSC Adv.* 2022;12(23):14729-14739. doi:10.1039/D2RA01673G
2. Owuamanam S, Cree D. Progress of bio-calcium carbonate waste eggshell and seashell fillers in polymer composites: A Review. *J Compos Sci.* 2020;4(2):70. doi:10.3390/jcs4020070
3. Minakshi M, Visbal H, Mitchell DRG, Fichtner M. Bio-waste chicken eggshells to store energy. *Dalton Trans.* 2018;47(47):16828-16834. doi:10.1039/C8DT03252A
4. Rahmayanti M, Fatimah I, Yahdiyani Ikhsani A, Nur Azizah D. The potential of calcium oxide nanocatalyst from chicken eggshells for biodiesel production using chicken fat waste. *Inorg Chem*

Commun. 2024;165:112604. doi:10.1016/j.inoche.2024.112604

5. Hargis CW, Chen I, Wang Y, Maraghechi H, Gilliam RJ, Monteiro PJM. Microstructure development of calcium carbonate cement through polymorphic transformations. *Cem Concr Compos*. 2024;153:105715. doi:10.1016/j.cemconcomp.2024.105715
6. Janik W, Kluska D, Staniek N, et al. Advantageous effect of calcium carbonate and chestnut extract on the performance of chitosan-based food packaging materials. *Ind Crop Prod*. 2024;219:119088. doi:10.1016/j.indcrop.2024.119088
7. Galotta A, Rubenis K, Locs J, Sglavo VM. Dissolution-precipitation synthesis and cold sintering of mussel shells-derived hydroxyapatite and hydroxyapatite/chitosan composites for bone tissue engineering. *Open Ceram*. 2023;15:100418. doi:10.1016/j.oceram.2023.100418
8. El Hayek J, Belaid H, De Saint Cyr LC, et al. 3D printed bioactive calcium silicate ceramics as antibacterial scaffolds for hard tissue engineering. *Mater Adv*. 2024;5(8):3228-3246. doi:10.1039/D3MA01088K
9. Mariyam M, Sunarintyas S, Yuliatun L, Irnawati D, Hatmanto AD, Nuryono N. Physicochemical and antibacterial properties of ZnO/chitosan-modified mineral trioxide aggregate composites. *CSCEE*. 2024;9:100749. doi:10.1016/j.cscee.2024.100749
10. Mariyam M, Sunarintyas S, Nuryono N. Improving mechanical, biological, and adhesive properties of synthesized mineral trioxide aggregate by adding chitosan. *Inorg Chem Commun*. 2023;149:110446. doi:10.1016/j.inoche.2023.110446
11. Pei Y, Chen P, Li S, Wang J. Producing amorphous calcium carbonate using waste Ca-rich solution generated through the bio-leaching of slag. *Sustain Chem Pharm*. 2023;36:101333. doi:10.1016/j.scp.2023.101333
12. Fa'izzah M, Widjijono W, Kamiya Y, Nuryono N. Synthesis and characterization of white mineral trioxide aggregate using precipitated calcium carbonate extracted from limestone. *KEM*. 2020;840:330-335. doi:10.4028/www.scientific.net/KEM.840.330
13. Salavati-Niasari M, Sabet M, Fard ZA, Saberyan K, Mostafa Hosseinpour-Mashkani S. Synthesis and characterization of calcium carbonate nanostructures via simple hydrothermal method. *Syn React Inorg Met-Org Nano-Met Chem*. 2015;45(6):848-857. doi:10.1080/15533174.2013.862643
14. Liendo F, Arduino M, Deorsola FA, Bensaid S. Factors controlling and influencing polymorphism, morphology and size of calcium carbonate synthesized through the carbonation route: A review. *Powder Technol*. 2022;398:117050. doi:10.1016/j.powtec.2021.117050
15. Di Marzio L, Borrego-Sánchez A, Felaco M, et al. Praziquantel-loaded calcite crystals: Synthesis, physicochemical characterization, and biopharmaceutical properties of inorganic biomaterials for drug delivery. *J Drug Deliv Sci Technol*. 2022;68:103021. doi:10.1016/j.jddst.2021.103021
16. Bikharudin, A., Sutarno, Kamiya, Y., N. Nuryono, Green preparation of precipitated calcium carbonate from limestone without calcination step, *AIP Conf. Proc*. 2553, 020038 (2022). doi:10.1063/5.0111595
17. Spelta JSDO, Galdino AGDS. Bioceramic composite: Hen's eggshell characterization and main applications. *Ifes Ciência*. 2018;4(1):9-20. doi:10.36524/ric.v4i1.323
18. Chen PC, Tai CY, Lee KC. Morphology and growth rate of calcium carbonate crystals in a gas-liquid-solid reactive crystallizer. *Chem Eng Sci*. 1997;52(21-22):4171-4177. doi:10.1016/S0009-2509(97)00259-5
19. Altiner M, Top S, Kaymakoğlu B. Ultrasonic-assisted production of precipitated calcium carbonate particles from desulfurization gypsum. *Ultrason Sonochem*. 2021;72:105421. doi:10.1016/j.ultsonch.2020.105421
20. Berdonosov SS, Znamenskaya IV, Melikhov IV. Mechanism of the vaterite-to-calcite phase transition under sonication. *Inorg Mater*. 2005;41(12):1308-1312. doi:10.1007/s10789-005-0307-6
21. Amin Alavi M, Morsali A. Ultrasonic-assisted synthesis of $Ca(OH)_2$ and CaO nanostructures. *J Exp Nanosci*. 2010;5(2):93-105. doi:10.1080/17458080903305616
22. Ryu MY, You KS, Ahn JW, Kim H. Effect of the pH and basic additives on the precipitation of calcium carbonate during carbonation reaction. *Resources Processing*. 2007;54(1):14-18. doi:10.4144/rpsj.54.14
23. Tizo MS, Blanco LAV, Cagas ACQ, et al. Efficiency of calcium carbonate from eggshells as an adsorbent for cadmium removal in aqueous solution. *Sustain Environ Res*. 2018;28(6):326-332. doi:10.1016/j.serj.2018.09.002
24. Ismaiel Saraya MES, Rokbaa HHAEL. Formation and stabilization of vaterite calcium carbonate by using natural polysaccharide. *ANP*. 2017;06(04):158-182. doi:10.4236/anp.2017.64014

25. Neumann M, Epple M. Monohydrocalcite and its relationship to hydrated amorphous calcium carbonate in biominerals. *Eur J Inorg Chem*. 2007;2007(14):1953-1957. doi:10.1002/ejic.200601033
26. Chakrabarty D, Mahapatra S. Aragonite crystals with unconventional morphologies. *J Mater Chem*. 1999;9(11):2953-2957. doi:10.1039/a905407c
27. Toffolo MB, Regev L, Dubernet S, Lefrais Y, Boaretto E. FTIR-based crystallinity assessment of aragonite–calcite mixtures in archaeological lime binders altered by diagenesis. *Minerals*. 2019;9(2):121. doi:10.3390/min9020121
28. Addadi L, Raz S, Weiner S. Taking advantage of disorder: amorphous calcium carbonate and its roles in biomineralization. *Adv Mater*. 2003;15(12):959-970. doi:10.1002/adma.200300381
29. Maisyarah AO, Shofiyani A. Sintesis CaO dari cangkang kerang ale-ale (*Meretrix meretrix*) pada suhu kalsinasi 900ºC. Jurnal Kimia Khatulistiwa. 2019;8(1):32-35. ISSN 2303-1077
30. Ma M, Yan Y, Qi C, et al. Symmetry-breaking assembled porous calcite microspheres and their multiple dental applications. *Sci China Materials*. 2017;60(6):516–528. doi:10.1007/s40843-017-9038-5
31. Jimoh OA, Ariffin KS, Hussin HB, Temitope AE. Synthesis of precipitated calcium carbonate: A review. *Carbonates Evaporites*. 2018;33(2):331-346. doi:10.1007/s13146-017-0341-x
32. Boulos RA, Zhang F, Tjandra ES, Martin AD, Spagnoli D, Raston CL. Spinning up the polymorphs of calcium carbonate. *Sci Rep*. 2014;4(1):3616. doi:10.1038/srep03616